Reprinted from "Surfactant Adsorption and Surface Solubilization",
R. Sharma, ed. ACS Symposium Series 615, p. 104-137, 1995

Chapter 7

Spectroscopic Characterization of Surfactant and Polymer Solloids at Solid–Liquid Interfaces

P. Somasundaran, S. Krishnakumar, and Joy T. Kunjappu

Langmuir Center for Colloids and Interfaces, Henry Krumb School of Mines, Columbia University, New York, NY 10027

Adsorbed surfactant and polymer layers play a major role in several key industrial operations such as flocculation/dispersion,ceramic processing, lubrication flotation and detergency. Much work has been done to understand the physico-chemical interactions that govern the formation of colloidal layers adsorbed on surfaces (*solloids*). The structure of these layers plays a critical role in determining interfacial properties and information on such structures, particularly at microscopic and molecular levels , can be helpful for controlling the behavior of the systems. We have recently adapted fluorescence, electron spin resonance, Fourier transform infrared, and excited-state resonance Raman spectroscopic techniques to obtain information on microstructure of adsorbed layers on a molecular level. In-situ characterization techniques that have been used recently for examining the adsorbed layers at the solid-liquid interface are reviewed here. Effects of surfactant and polymer structure, pH, and their synergistic effects on the evolution and properties of the adsorbed layer are discussed.

Adsorption of surfactants and polymers at the solid-liquid interface is a key phenomena in many important processes such as flocculation, flotation, dispersion, and stabilization *(1)*. These applications are a sequel to the modification of the solid surface by the adsorbates in terms of the electrical and allied processes. Optimum performance of these processes is possible by a detailed understanding of the adsorbates at the solid-liquid interface and the related structure-performance relationship of these species.

In this article, we discuss some of the advanced techniques and methodologies that we have used recently for investigating the microstructure of the adsorbed monomeric and polymeric aggregates at the solid-liquid interface, which are known

0097–6156/95/0615–0104$15.50/0

as solloids (surface colloids). We have investigated the complex dependence of the adsorbed layer structures on the processes of dispersion, flocculation and flotation. We have used mainly the techniques of fluorescence emission, electron spin resonance, Fourier transform infrared, and excited state Raman spectroscopy to delineate the microstructure of the adsorbed layers of surfactant and polymeric aggregates.

We first give a description of the basic principles of the above spectroscopic techniques as used in our studies. This description is followed by a discussion of the individual systems comprising of surfactants, polymers, mixed surfactants and surfactant-polymer aggregates at various solid-solution interfaces. These interfaces include alumina and silica in aqueous and non-aqueous media.

Techniques

Fluorescence Spectroscopy. Fluorescence emission is the radiative emission of light by an excited molecule returning to its ground state energy level. This phenomenon bears a wealth of information on the environment of the light absorbing species and has been exploited for a long time for exploring the solution behavior of surfactants. Parameters of fundamental importance in fluorescence emission are 1) emission maximum (wavelength of maximum intensity), 2) quantum yield of fluorescence (emission efficiency measured as intensity) and 3) fluorescence life-time (time taken by the excited state to decay to 1/e of its initial value).

The fluorescence measurements are generally carried out by a steady state fluorescence spectrofluorometer and lifetime of fluorescence by time resolved fluorescence lifetime instrument *(2)*. The dependence of fluorescence intensity and life-time on the physicochemical environment of the fluorescing molecule has been well documented *(3)*. Such data for micellar photochemistry has been used to understand the microenvironment within micelles *(4)*. We have recently adapted this technique as a tool to investigate the adsorbed layer structures of surfactants on solids to obtain information on the *micropolarity, microviscosity* of the probe environment and the *aggregation number* of the surfactant adsorbed at the interface. To determine the micropolarity, a fluorescent molecule like pyrene, which possesses a highly structured fluorescence spectrum whose vibrational lines are susceptible to intensity fluctuations brought on by polarity changes of the medium, is used. This empirical knowledge has been found to be of universal applicability and used widely to investigate the micropolarity of micelles. A properly resolved fluorescence spectrum of pyrene in fluids exhibits five vibronic bands in the region from 370 to 400 nm. The intensities of the first (I_1) and the third (I_3) are found to be particularly sensitive to the changes in the probe environment. The ratio of these peaks (I_3/I_1), sometimes referred to as the polarity parameter, changes from ~ 0.6 in water to a value greater than unity in hydrocarbon media.

The dynamics of fluorescence emission of pyrene has been previously studied in homogeneous and micellar solutions using time resolved fluorescence spectrometry *(5)*. While the decay kinetics of monomer and excimer emission may be derived directly for a homogeneous solution (continuous medium), statistical methods are to be applied to arrive at similar kinetics in aggregated micellar ensembles. This stems from a need to recognize the possibility of random multiple occupancy of the probe in the

aggregates which affects the excimer forming probability within the aggregate. If the micellar system is viewed as a group of individual micelles with n probes, P_a the average number of probes per micelle, may be related to n, by Poisson statistics through the relation

$$P_a = n^n \exp(-n)/n! \quad (1)$$

This model yields the following relation for the time dependence of monomer emission

$$I_{m(t)} = I_{m(0)} \exp [-k_o t + n(\exp (-k_e t)-1)] \quad (2)$$

where k_0 is the reciprocal lifetime of excited pyrene in the absence of excimer formation, k_e is the intra micellar encounter frequency of pyrene in excited and ground states, and $I_{m(0)}$ and $I_{m(t)}$ represent the intensity of monomer emissions at time zero and time t respectively. Knowing n, one can calculate aggregation number N using the expression

$$n = [P]/[Agg] = [P]\, N/ ([S] - [S_{eq}]) \quad (3)$$

where [P] is the total pyrene concentration, [Agg] is the concentration of the aggregates and [S] - $[S_{eq}]$ is the concentration of the adsorbed surfactant.

Electron Spin Resonance Spectroscopy (ESR). Molecular species with a free electron possesses intrinsic angular momentum (spin), which in an external magnetic field undergoes Zeeman splitting. For a system with S=1/2, two Zeeman energy levels are possible whose energy gap (Δ E) is given by

$$\Delta E = h\nu = gBH_o \quad (4)$$

where ν is the frequency of the electromagnetic radiation corresponding to ΔE, g is a proportionality constant, B is the Bohr magneton (natural unit of the magnetic moment of the electron), and H_0 is the applied magnetic field.

The magnetic moment of the free electron is susceptible also to the secondary magnetic moments of the nuclei and thus the Zeeman splitting will be superimposed by the hyperfine splitting which brings about further splitting of the absorption signal. The hyperfine splitting pattern depends on the spins and the actual number of the neighboring nuclei with spins. If the electron is in the field of a proton (s=1/2, where s is the spin quantum number) then the ESR spectrum would yield two lines of equal intensity and similar interaction with a nucleus, as in nitrogen (s=1), would produce a triplet of equal intensity. The line shapes of ESR signals are subject to various relaxation processes (spin lattice and spin-spin relaxations) occurring within the spin system as well as anisotropic effects due to the differentially oriented paramagnetic centers being acted upon by an external magnetic field *(6)*. These effects result in a broadening of the absorption lines. Three types of ESR studies can be applied to probe surfactant microstructures - spin probing, spin labeling and spin trapping *(7)*. In the

spin-probing technique, a molecule with a spin is externally added to the system, whereas in spin labeling a spin bearing moiety forms a part of the molecule through covalent bonding. The spin trapping technique is mainly used for the identification of radicals produced thermally, photochemically or radiolytically by trapping the radical through chemical reactions with a spin trap (like butyl nitroxide) and converting the radical to a free radical which can be examined by ESR. This technique has been used widely to study micellization of different surfactants in both aqueous and non-aqueous media *(8),(9),(10)*. This has also been used to study the exchange kinetics and solubilization sites in water-in-oil microemulsions *(11)* . ESR studies as applied to micellar systems rely on the sensitivity of a free radical probe to respond to its microenvironment.

Information on micropolarity and microviscosity can be obtained by measuring the hyperfine splitting constant A_N and the rotational correlation time τ. The latter is the time required for a complete rotation of the nitroxide radical about its axis. Its value can be defined as the time required for the nitroxide to rotate through an angle of one radian. The rotational correlation time (τ) measured from the ESR spectrum is reflective of the probe mobility and can be used to monitor the changes in microviscosity of the adsorbed layer brought about as a result of adsorption followed by close packing of molecules in the adsorbed layer. The hyperfine splitting constant (A_N) that can also be measured from the spectrum, changes as a function of the environment polarity and hence yields information on the formation of different microdomains at the interface as a result of adsorption. In the case of slow anisotropic motion the observed changes in the spectrum can be quantified by using the concept of order parameter S which can be calculated from the spectrum using the following equation

$$S = \frac{(A_{//}-(A_1(meas)-C))}{(A_{//}-2(A_1(meas)-C))} \quad where \quad C = (1.45-0.019(A_{//}-A_1(meas))) \quad gauss \qquad (5)$$

and $A_{//}$ and A_1 are the hyperfine splittings measured from the spectra. The order parameter is usually a parameter of molecular motion and varies between 0 (low order) and 1(high order).

Infrared Spectroscopy (IR). The vibrational frequencies of bonds in a molecule correspond to the infrared region of the electromagnetic spectrum. Different groups in a molecule possess characteristic absorption frequencies which serve as their identification marks. Moreover, these frequencies are related to the bond strength, bond energy and other related parameters. In the case of a diatomic molecule, the stretching frequecy v is expressed as,

$$\nu = 1/(2\pi c)\sqrt{(k/\mu)} \qquad (6$$

where k is the force constant, c the velocity of light, and μ, the reduced mass which is equal to$(m_1+m_2)/m_1m_2$, m_1 and m_2 being the masses of the atoms forming the bond *(12)*

A prerequisite for the absorption of infrared radiation by a molecule is that the concerned vibration should cause a change in its dipole moment. Both the stretching and bending vibrations are useful for the identification of the bonding characteristics. The frequency positions and the frequency intensities help in the qualitative detection and the quantitative estimation respectively.

The common IR sampling methods such as KBr pelletting, mujol mulling, etc. cannot be applied to an aqueous environment. The analysis of solid samples has been accelerated by the use of attenuated total reflectance technique (ATR). In this mode, the powdered sample or the slurry is smeared on an internal reflection element (IRE). The evanescent field of the IR light undergoing multiple internal reflections samples the material adhering onto the IRE and gets attenuated collecting information on the vibrational aspects of the material. Equations are available which relate the adsorption density (Γ) of surfactants quantitatively to the parameters of IRE and IR light exemplified as follows *(13)*,

$$\Gamma = [\{A/(l/\cot\theta) - \varepsilon C_b d_e\}] / 1000\varepsilon\,(2d_e/d_p) \qquad (7)$$

where A = integrated absorbance (cm^{-1}), l = IRE length, t = IRE thickness, ε = molar absorptivity of surfactant ($l/(cm^2.mol)$), C_b = surfactant bulk concentration (mol/l), d_p = depth of penetration, d_e = effective depth, and θ = incident angle of light on IRE (degrees).

Raman Spectroscopy. Raman spectroscopy is essentially a scattering technique giving information on the vibrational modes of a molecule. Those vibrations causing a polarizability change of a molecule are Raman active. Raman spectroscopy has an edge over infrared spectroscopy since it is ideal in an aqueous environment and versatile in its ease of sample handling.

The Raman process (inelastic scattering) is inherently weak in sensitivity due to its low cross section ($\sim 10^{-6}$). An inelastic impact of the molecule with the light quantum results in transferring the vibrational energy from the light quantum to the molecule (Stokes process) or from the molecule to the light quantum (anti-Stokes process). The electric field of the light induces in the molecule a dipole moment μ' which is related to the field strength E and polarizability α of the molecule according to the equation

$$\mu' = \alpha E \qquad (8)$$

The directional dependence of the polarizability is described by a tensor which becomes symmetrical for a non-chiral molecule. Quantum mechanical treatment provides a good estimate of the intensities of the Stokes and anti-Stokes lines, though the classical picture does not provide a resonable estimate.

The earlier Raman studies have been carried out under continuous wave light. With the advent of lasers, both continuous wave and pulsed lasers are used for collecting Raman spectra. To enhance the intensity of Raman lines, the excitation can be localized to a narrow absorption band (Resonance Raman Scattering). The intensity problem is overcome in a few cases by the Surface Enhanced Raman Spectroscopy

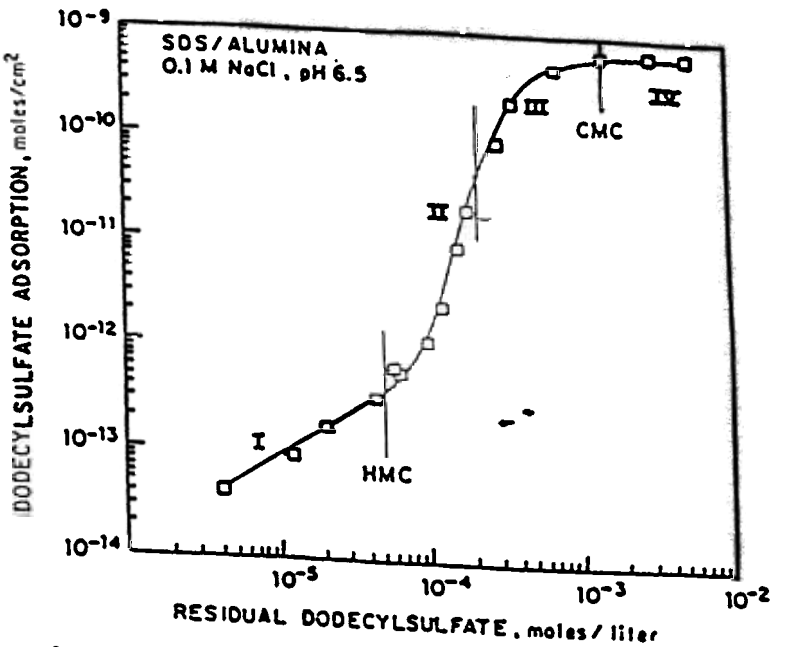

Figure 1. Adsorption isotherm of sodium dodecylsulfate (SDS) on alumina at pH 6.5 in 10^{-1} kmol/m^3 NaCl.

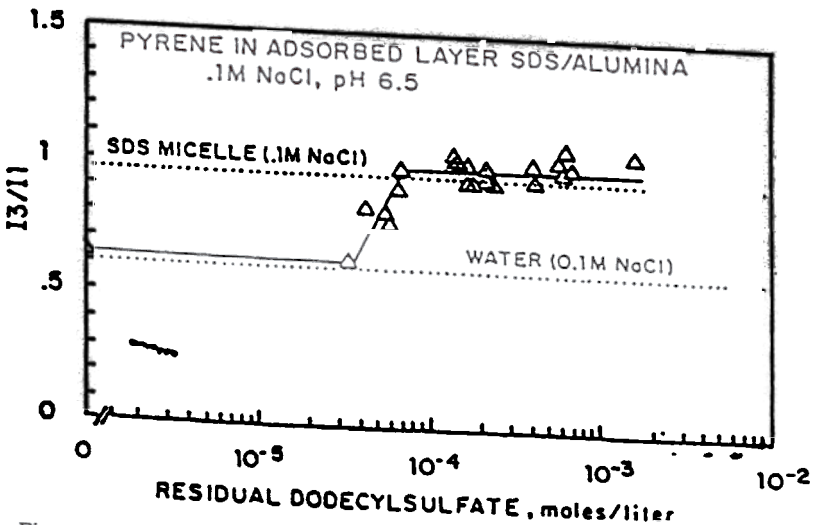

Figure 2. I_3/I_1 fluorescence parameter of pyrene in sodium dodecylsulfate (SDS) in alumina slurries. (Reproduced with permission from ref. 20. Copyright 1987, Academic Press)

parameter is fairly constant throughout most of the Region III and above and hence seems to be independent of the surface coverage.

Information on microviscosity of the adsorbed layer is obtained by studying the excimer (excited dimer) forming capabilities of suitable fluorescent molecules like 1,3-dinaphthyl propane. The excimer, which is a complex of a ground state and an excited state monomer, has a characteristic emission frequency. The intramolecular excimer formation is a sensitive function of the microviscosity of its local environment. This property, expressed as the ratio of the monomer to excimer yield (I_m/I_e) for 1,3-dinaphthyl propane, is determined (Figure 3) for the solution and for the adsorbed layer for the various regions of the adsorption isotherm *(21)*. These are then compared to the I_m/I_e values of DNP in mixtures of ethanol and glycerol of known viscosities. Based on the I_m/I_e values of DNP for ethanol-glycerol mixtures, a microviscosity value of about 100 cP is obtained for the adsorbed layer compared to a value of 8 cP for micelles. A higher value of microviscosity in the solloid as reported by DNP is indicative of a highly condensed surfactant assembly.

A kinetic analysis based on the relation of the decay profiles of pyrene in the adsorbed layer for different regions of the alumina/dodecylsulfate adsorption isotherm yielded the aggregation numbers marked in Figure 4 for dodecyl sulfate solloids (20). These results yield a picture of the evolution of the adsorbed layer. The aggregates in Region II appear to be of relatively uniform size while in Region III there is a marked growth in the aggregate size. In Region II, the surface is not fully covered and some positive sites are still available for further adsorption. Since the aggregation number is fairly constant in Region II, further adsorption in this region can be considered to occur by the formation of more aggregates but of the same size. The transition from Region II to III corresponds to the isoelectric point of the solid, and adsorption in region III is proposed to occur through the growth of existing aggregates rather than the formation of new ones due to lack of positive adsorption sites. This is possible by the hydrophobic interaction between the hydrocarbon tails of the already adsorbed surfactant molecules and the adsorbing ones. The new molecules adsorbing at the solid-liquid interface can be expected to orient with their ionic heads towards the water, as supported by the hydrophobicity studies*(22)*, since the solid particles possess a net negative charge under these conditions. A schematic representation of the adsorption by lateral interactions is given in Figure 5.

These studies were complemeted by using ESR to further investigate changes in microviscosity within the adsorbed layer using three isomeric stable free radicals 5-, 12- and 16- doxyl stearic acids as the spin labels. These spin labels were co-adsorbed individually on the alumina along with the main adsorbate, sodium dodecylsulfate, and the main regions of the isotherm were investigated. The hyperfine splitting constants of 16-doxyl stearic acid measured in dodecyl sulfate solloids (15.0G) are indicative of a less polar environment in comparison to its value for water (16.0G) and SDS micelles (15.6G). Similarly microviscosities were estimated from τ measurements and calibrated against τ measured in ethanol-glycerol mixtures (Figure 6). These give reasonably high values for the solloids in reference to the values for water. Three different microviscosities were obtained using different probes indicating that the nitroxide group in each case experienced a different viscosity within the solloid. These observations may be explained by assuming a model for the adsorption of the probe in

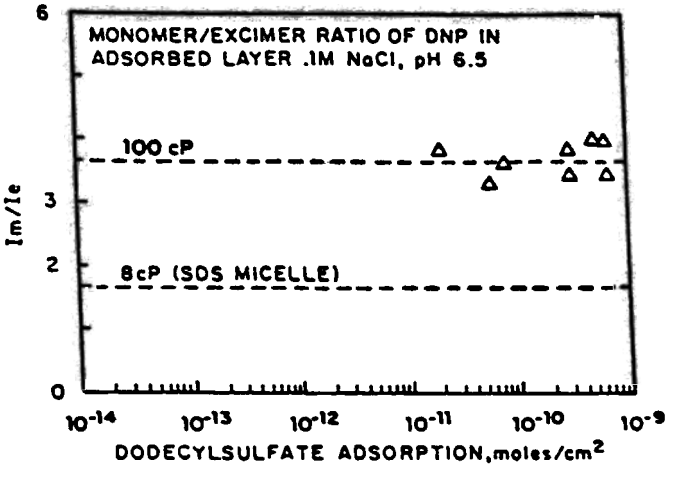

Figure 3. Monomer to excimer ratio (I_m/I_e) of dinaphthyl propane (DNP) in SDS-alumina slurries as a function of SDS adsorption density. The viscosities refer to those of ethanol-glycerol mixtures which give a similar I_m/I_e ratio for DNP. (Reproduced with permission from ref. 20. Copyright 1987, Academic Press)

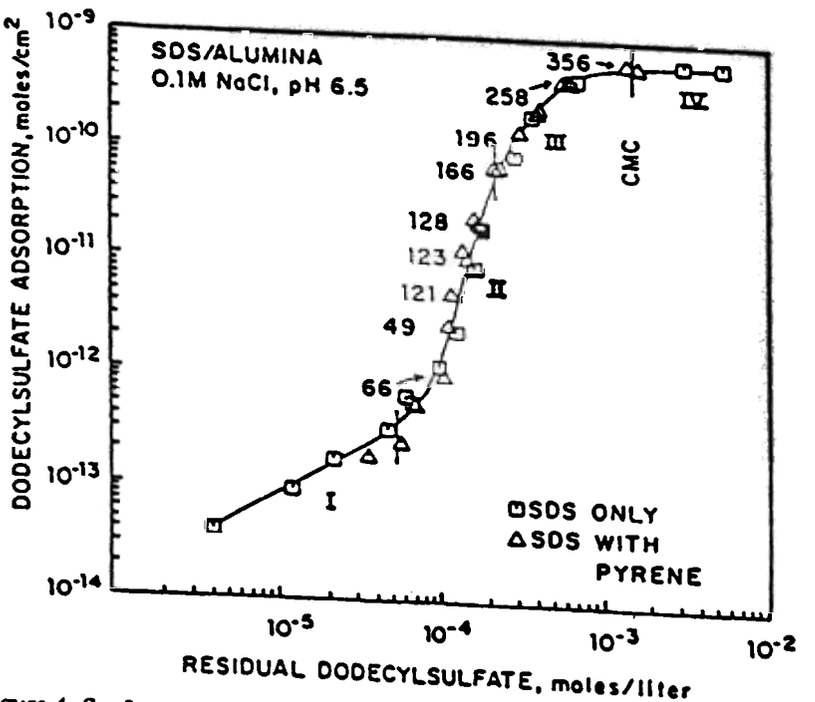

Figure 4. Surfactant aggregation numbers determinined for various adsorption densities (average number is indicated). (Reproduced with permission from ref. 20. Copyright 1987, Academic Press)

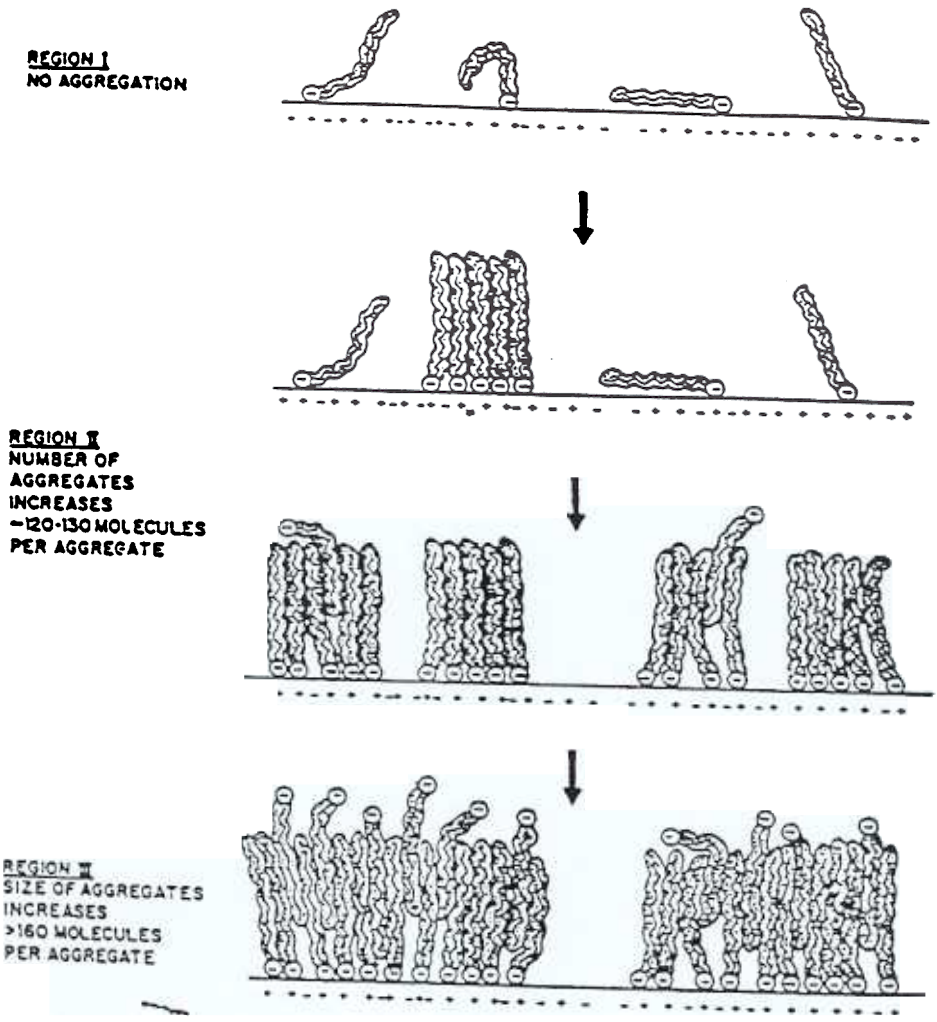

Figure 5. Schematic representation of the correlation of surface charge and the growth of aggregates for various regions of the adsorption isotherm depicted in Figure 1. (Reproduced with permission from ref. 20. Copyright 1987, Academic Press)

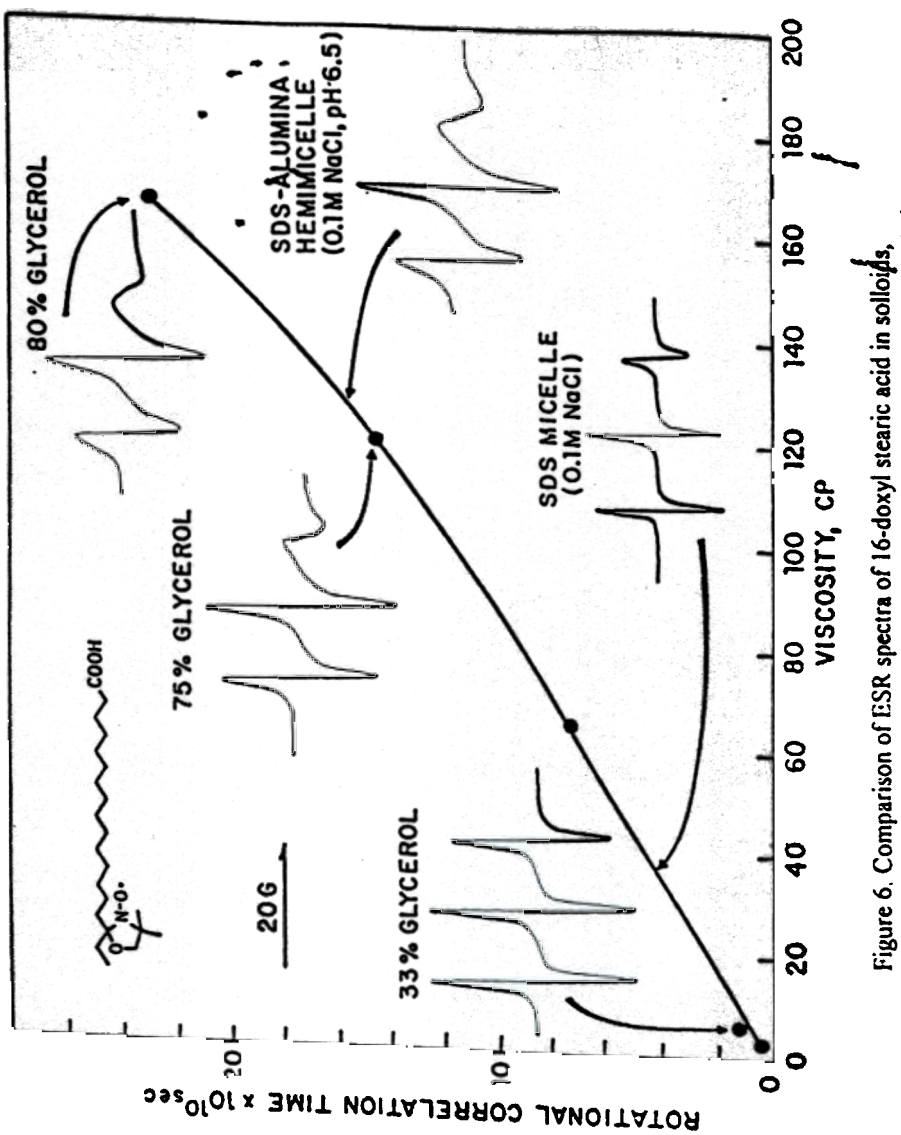

Figure 6. Comparison of ESR spectra of 16-doxyl stearic acid in solloids, micelles and ethanol-glycerol mixtures and corresponding rotational correlation times and viscosities. (Adapted from ref. 23)

which the carboxylate group is bound to the alumina surface. Such a model would require greater mobility of the nitroxide moiety near the SDS/H_2O interface (as in the 16-doxyl stearic acid case) and less mobility of the 12-doxyl and 5-doxyl probes *(23),(24)*. This work is the first reported indication of variations in microviscosity within a surfactant solloid as estimated by any known technique.

The alumina/dodecylsulfate system has also been probed by excited state resonance Raman Spectroscopy using Tris(2,2'-bipyridyl) ruthenium (II) chloride [$Ru(bpy)_3^{2+}$] as a reporter molecule*(25)*. It has been shown that ruthenium polypyridyl complexes serve as excellent photophysical probes for biopolymers like nucleic acids. The excited state of $Ru(bpy)_3^{2+}$ shows strong resonance enhanced Raman transitions when probed at 355 nm. Furthermore, it has been shown that binding of this ion to clay particles results in substantial changes in the ground-state transitions of the excited state-resonance Raman spectrum. For these reasons this probe was chosen to study the solloids formed at the alumina-water interface with excited-state resonance Raman spectroscopy. The third harmonic of a Nd-YAG laser excited and scattered the $Ru(bpy)_3^{2+}$ molecules at a pulse energy of 5 mJ, pulse width of 6 ns, and a wavelength of 354.5 nm. The excited state Raman spectrum of $Ru(bpy)_3^{2+}$ consisting of 14 lines (7 lines each from the ground and the excited states) was calibrated using an authentic spectrum.

Raman spectra of $Ru(bpy)_3^{2+}$ above the CMC show frequency shifts as well as intensity changes as compared to its spectrum in water. These transitions can be attributed to the perturbation of the excited state by the SDS micelles. Excited state resonance Raman spectrum of this probe in various regions of adsorption isotherm for the alumina/SDS system is shown in Figure 7. The spectrum of $Ru(bpy)_3^{2+}$ on alumina in the absence of SDS is very much similar to its spectrum in water both in terms of frequencies and relative intensities. This trend is continued into region II, where the solloid aggregation process begins. In regions III and IV, the Raman spectrum shows significant changes. The frequency shifts are more pronounced than in the case of micelles. A plot of change in wave numbers for some of the lines in the four different regions of the adsorption isotherm is shown in Figure 8. The changes in Raman frequency and intensity assume substantial significance in the transition regions II and III onwards only. This could be due to the change of net charge on the alumina surface from positive to negative. The favorable net negative charge enhances the adsorption of the probe at the solid-liquid interface. Accordingly, no adsorption of $Ru(bpy)_3^{2+}$ was observed when the supernatants were analyzed in Region I and Region II or in the absence of SDS. These results indicate that adsorption of $Ru(bpy)_3^{2+}$ onto alumina becomes significant only close to the isoelectric point. The transitions at 1213, 1286 and 1428 cm^{-1} show significant increments and these trends clearly suggest the probe adsorption on to the solloids. Also it was seen that the 1286 peak shifted to 1281 in the presence of solloids while it was practically unchanged in the sodium dodecylsulfate micelles. It may be speculated that $Ru(bpy)_3^{2+}$ may be sensing different environments within the SDS micelles and the alumina/SDS solloids. Implicit in these results is also the potential of the time resolved Raman spectroscopy as a powerful diagnostic tool to explore the solid - liquid interface.

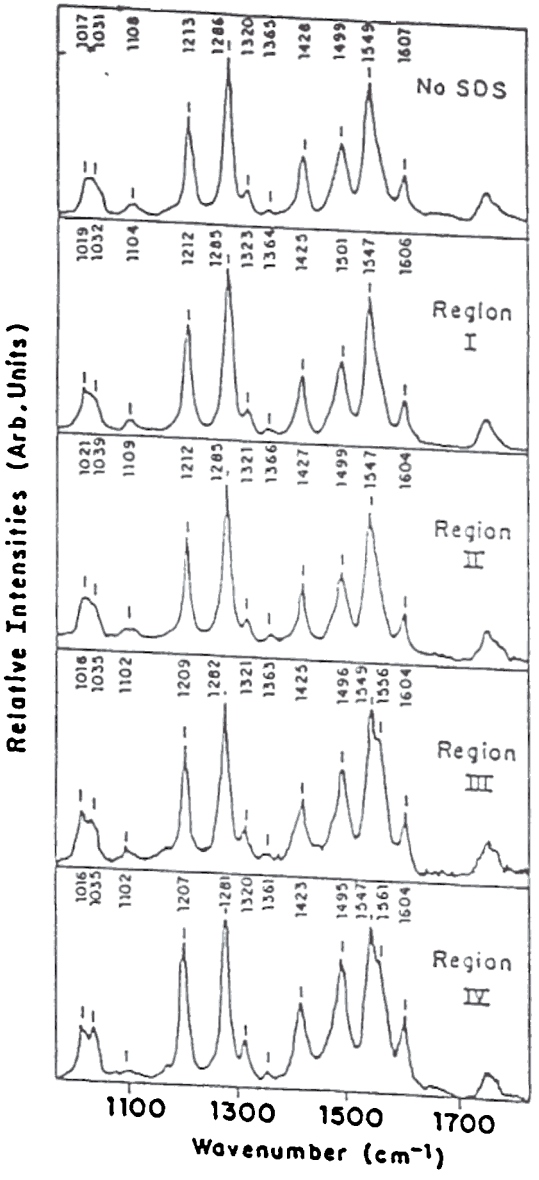

Figure 7. Resonance Raman spectrum of $Ru(bpy)_3^{2+}$ for various regions of the alumina/SDS adsorption system. (Adapted from ref. 25)

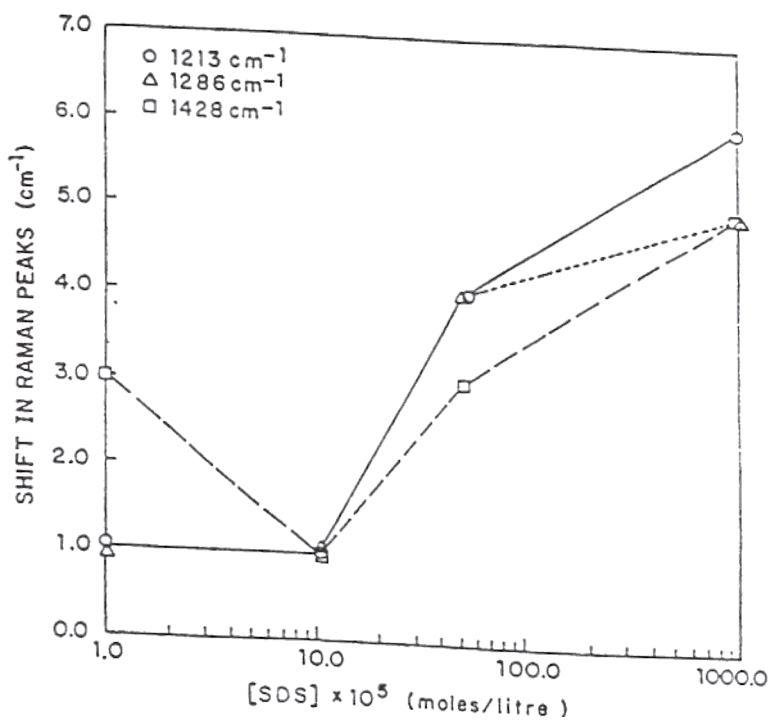

Figure 8. Frequency shifts of resonance Raman lines of $Ru(bpy)_3^{2+}$ as a function of SDS concentration for the alumina/SDS system. (Adapted from ref. 25)

Isomeric Surfactants at an Interface *(26)*. Studies of changes in the position of the sulfonate and the methyl groups on the aromatic ring of alkylxylenesulfonate showed a marked effect of such changes on the micellization and adsorption at the alumina/water interface. Fluorescence spectroscopy was used to probe the microstructure of the adsorbed layers in these systems. Adsorption isotherms for 4-(4-undecyl)-2,6-dimethylbenzenesulfonate (Para-1), 4-(4-undecyl)-2,5-dimethylbenzene sulfonate (Para-2) and 5-(4-undecyl)-2,4-dimethylbenzenesulfonate (Meta) on alumina from water and the I_y/I_i values along various regions of the isotherm are shown in Figure 9 and 10 respectively. At low adsorption densities the value of the polarity parameter, I_y/I_i, is ~ 0.6 and once the solloids form the value goes up to about 1. It can also be seen that there is no measurable difference among the polarities of the adsorbed layers of the three surfactants indicating that these layers in all three cases are structurally similar with minimum water penetration. Average aggregation numbers (determined using fluorescence decay) of the solloids increase from 17 to 76 with increase in adsorption in all the three cases (Figure 11). The aggregation numbers of the two paraxylene sulfonates are similar throughout the range studied. However, at higher adsorption densities, the aggregation number of the metaxylenesulfonate is lower than those of the paraxylenesulfonates. This suggests higher steric hindrance to the packing of the surfactant molecules in the solloids of the metaxylenesulfonate. Based on this evidence, the effect of change of functional groups on the aromatic ring of the alkylxylenesulfonates on adsorption can be attributed to the steric constraints to the packing of surfactant molecules in their aggregates.

Conformation of Aerosol-OT at Alumina-Cyclohexane Interface *(27),(28)*. Colloidal dispersions in non-aqueous media have a number of technological applications, but water is present in most of these cases and plays a major role in determining the dispersion behavior. The adsorption of Aerosol-OT, sodium bis(2-ethylhexyl) sulfosuccinate, on alumina was investigated using Infrared spectroscopy *(29)*. Figure 12 shows the IR spectrum of AOT adsorbed on alumina in cyclohexane along with the spectra for alumina and AOT. The spectrum does not show any new absorption bands or shifts in the existing bands on alumina or AOT due to the adsorption. This suggests that the adsorption proceeds via weak physical interaction. The effect of water on the stability of a colloidal suspension of alumina in cyclohexane in the presence of surfactant, Aerosol-OT is shown in Figure 13. A succession of flocculated, dispersed and flocculated states are observed as the amount of water added to the suspensions is increased. ESR studies were conducted using 7-doxyl stearic acid as a probe to get structural information on the adsorbed layer.

Figure 14 shows some of the spectra obtained at different water concentrations with 7-doxyl stearic acid coadsorbed with a full monolayer of Aerosol-OT on the alumina surface. The changes observed in the ESR line shape correspond to an increase in the probe mobility consistent with a decrease in the ordering of the probe environment. The calculated order parameter (eqn. 5) plotted as a function of water concentration is shown in Figure 15. It can be seen that as more water is added to the suspension the order parameter decreased until it reached a constant value of 0.75. These results are interpreted in terms of an increase in the probe lateral diffusion within the adsorbed surfactant layer. Such an increase in the probe lateral diffusion is realistic,

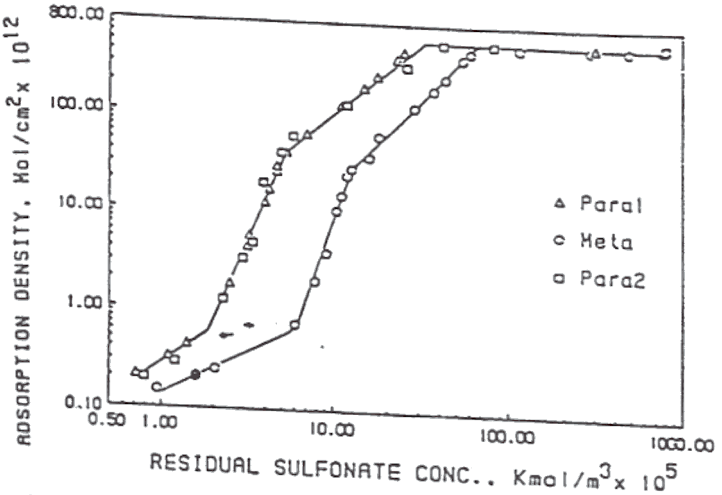

Figure 9. Adsorption of alkylxylene sulfonates on alumina. (Adapted from ref. 26)

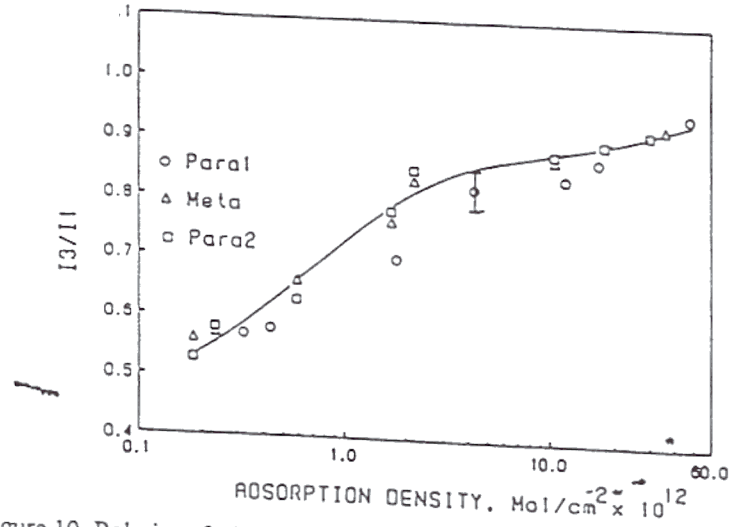

Figure 10. Polarity of adsorbed layers of alkylxylenesulfonates in terms of I_3/I_1 as a function of surfactants adsorption density. (Adapted from ref. 26)

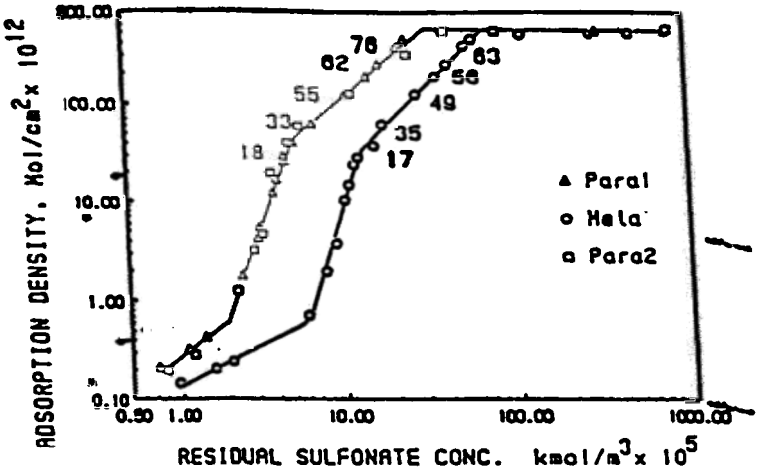

Figure 11. Aggregation numbers determined at different adsorption densities shown along the isotherm. (Adapted from ref. 26)

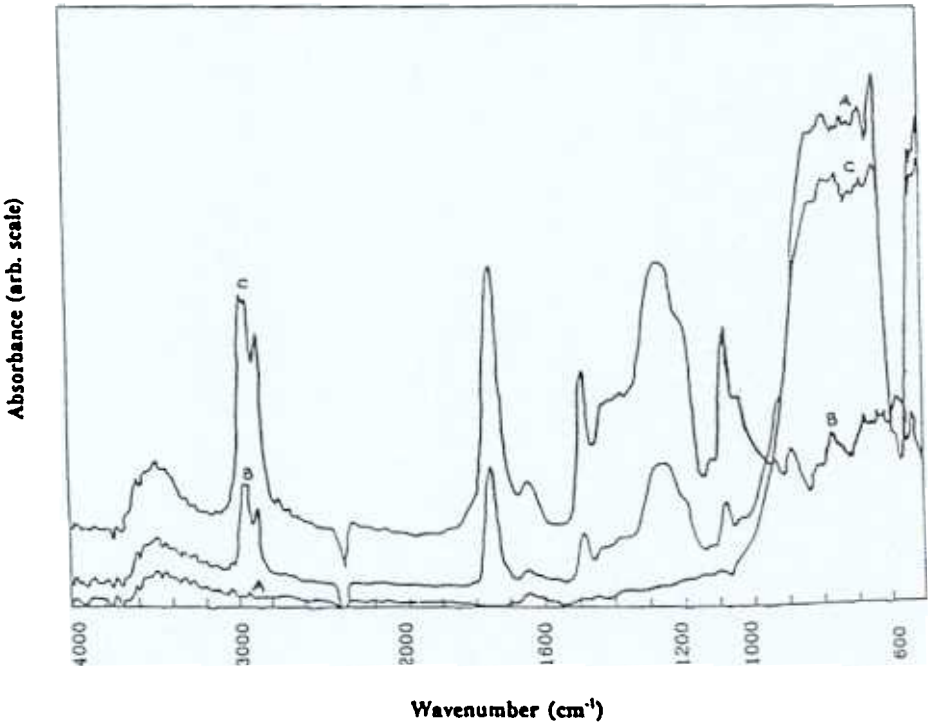

Figure 12. Infrared spectrum of (a) pure alumina (b) pure AOT and (c) AOT adsorbed on alumina. (Adapted from ref. 29)

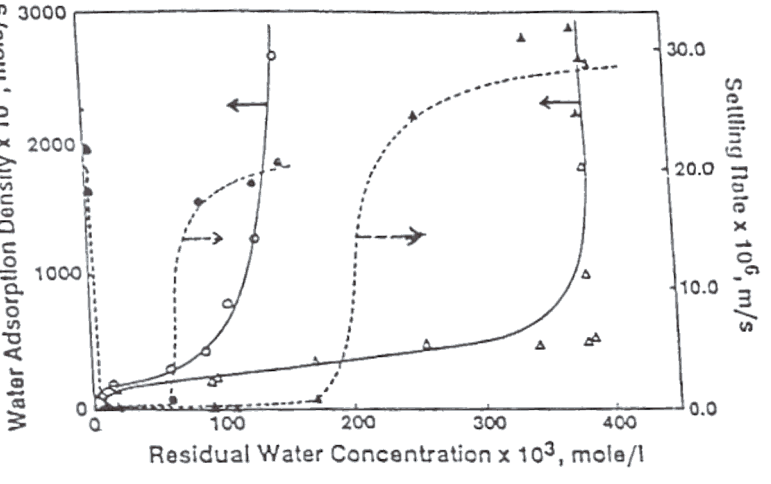

Figure 13. Effect of water on the alumina suspension stability at two different surfactant concentrations; solid symbols [AOT] = 8.5 x10^{-3} M/l and hollow symbols [AOT] = 26.5 x 10^{-3} M/l (dotted line): The corresponding water adsorption densities are also shown (solid line). (Adapted from ref. 28)

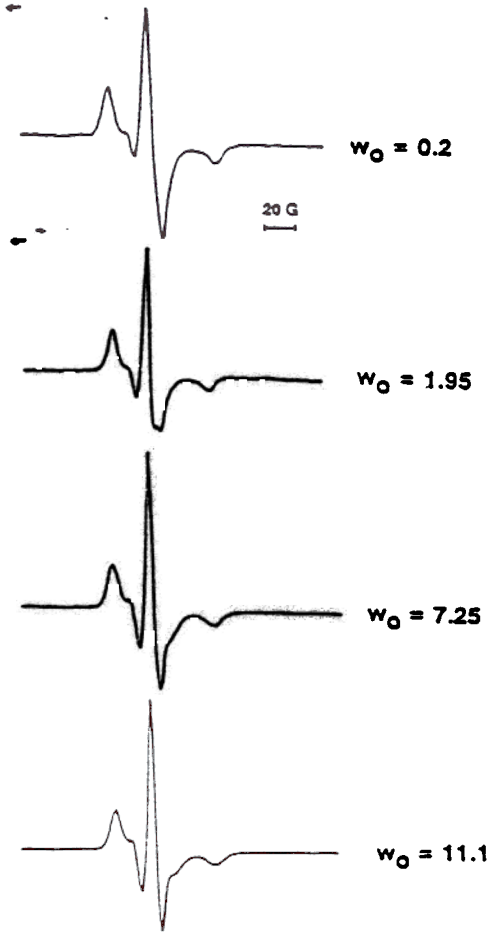

Figure 14. Effect of water on the ESR spectra of 7-doxyl stearic acid coadsorbed with a monolayer of Aerosol-OT at the alumina/cyclohexane interface. (Adapted from ref. 28)

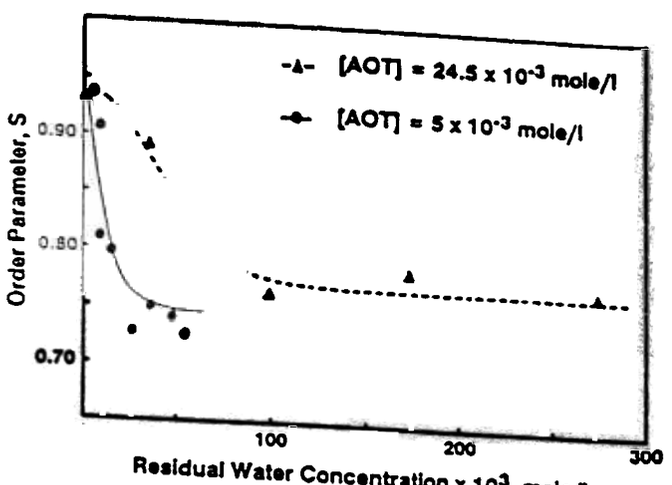

Figure 15 .Effect of water on the order parameter, S, calculated from the ESR spectra of 7-doxyl stearic acid coadsorbed with Aerosol OT at the alumina/cyclohexane interface.(Adapted from ref. 28)

considering the structural reorganization of the complex adsorbed layer when water is present at the interface. At low water concentrations, water molecules bind the carboxylic groups of the stearic acid molecules and the polar groups of Aerosol OT, directly to the hydroxyl groups of the alumina surface. This binding limits the ability of the probe to move within the adsorbed layer and is consistent with a model of localized adsorption where the adsorbed molecules have limited degrees of freedom. As the water adsorption density increases, the carboxylic groups of the probe molecules interact with water molecules not bound directly to the hydroxyl groups of the mineral surface. Similar interactions between the polar groups of Aerosol OT and water molecules are most likely, as a result of which the adsorbed layer can become loosely bound to the mineral surface. The molecular diffusion limited by the binding of the surfactant molecules at low water concentrations thus increases markedly as water adsorbs on particles.

Oleate on Dolomite and Francolite. FTIR spectroscopy in the ATR mode has been employed to investigate the surface precipitation phenomenon during the adsorption of oleate on Francolite and Dolomite. Near total flotation of the individual minerals could be achieved with oleate collector, a reagent used to induce surface hydrophobicity. Based on that, the flotation of binary mixtures attempted under restricted conditions of pH deemed to provide excellent selectivity based on the data for individual minerals. It was conjectured that the loss in selectivity of flotation of the above mixed minerals could be due to the alteration of the surface properties of the minerals due to the interactions between dissolved mineral species and the oleate resulting in surface and bulk precipitation. An FTIR experiment was performed in a Harrick's ATR liquid prism assembly with dolomite/oleate system. Dolomite shows a strong C=O stretching frequency of the carbonate group at 1488 cm^{-1}. Figure 16 shows the FTIR spectra of dolomite mixed with oleate at various concentrations of the latter. The dolomite peak is seen to diminish with increasing oleate concentration and a new peak characteristic of the oleate appears at a lower frequency. The decrease in the dolomite peak is attributed to direct oleate adsorption, formation of Ca and Mg oleate precipitates on the mineral surface and/or to the masking of carbonate groups on the mineral surface. This observation was in agreement with the results from depletion isotherms of the oleate and the dependence on the concentrations of the dissolved Ca^{2+} and Mg^{2+} species at the interface and in solution *(30)*.

Mixed Surfactants on Alumina. Most of the practical situations related to industrial processes such as enhanced oil recovery deal with mixed surfactant systems *(31)* arising either as contaminants or as deliberately added components to tune the surface properties. Mixed surfactants are considerably less expensive and readily available than pure components. Moreover, in mixed systems comprising ionic and non-ionic surfactants, the problem of precipitation is abated and greater salt tolerance is achieved.

While the solution properties of mixed surfactant systems have been addressed recently *(32)*, the nature of aggregation of mixed suractants on solids has been only scantly investigated. We have attempted recently to elucidate the microstructural properties of adsorbed layers of mixed surfactants on solids like alumina, silica and kaolinite by spectroscopic techniques to supplement the information gathered from

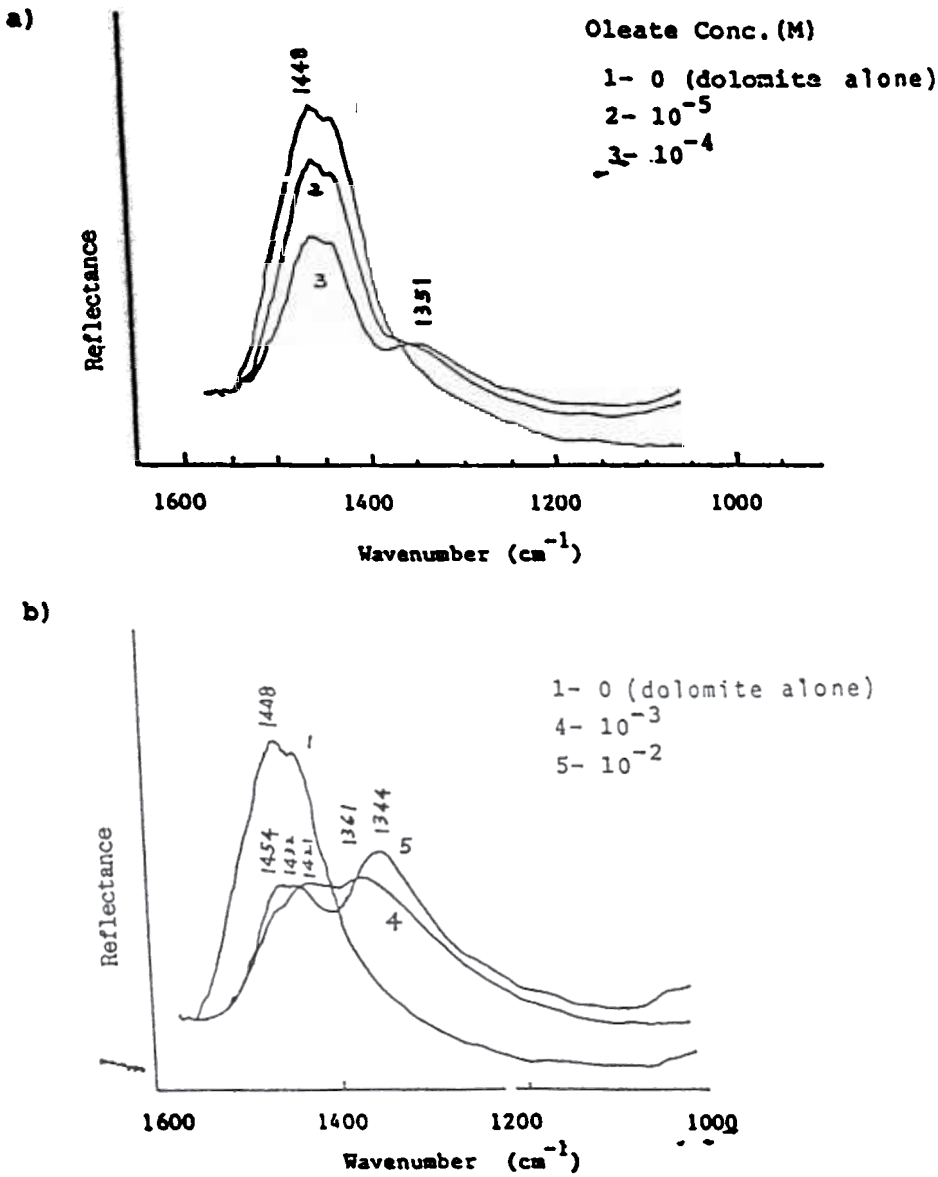

Figure 16. ATR spectra of dolomite slurry at different concentrations of oleate; (a) low concentration region, (b) high concentration region.

adsorption, microcalorimetry and allied studies *(33)*. The microstructures of sodium dodecylsulfate and dodecyloxyheptaethoxyl ethyl alcohol ($C_{12}EO_8$) layers on alumina were probed with pyrene. The polarity parameter measured at various points on the isotherm is shown in Figure 17. It is seen that the polarity parameter is nearly a constant along the isotherm, while the value in dodecylsulfate micelles is lower than that obtained for it at the alumina-water interface. This throws light on the compact nature of the adsorbed layers. Pyrene probing of the $C_9\phi EO_{40}$ (nonylbenzene derivative) aggregates on silica showed that no hydrophobic aggregates were formed at the solid-liquid interface.

Polymer/Solid Systems

Polymer Conformation in the Adsorbed State. Polymers can exist in different conformations both in solution and in the adsorbed state. The adsorption of polymeric materials onto solid surfaces can be quite different from the adsorption of small molecules in that the polymer adsorption is greatly influenced by the multifunctional groups that it possesses *(34)*. This stems from the widely varying sizes and configurations available for the polymer. In addition, macromolecules usually possess many functional groups each having a potential to adsorb on one or more given surfaces.

Among the polymeric materials, polyelectrolytes are the most important because of their participation in many biological processes and their utility in processes like dispersion, flocculation, adhesion and rheology. Polyacrylic acid (PAA) is chosen here as a model polyelectrolyte to gain insight into the adsorption behavior of polyelectrolytes in general. Such an understanding is important in acquiring effective control over processes of colloidal stabilization and flocculation.

Polyacrylic acid can exist in different conformations depending on the solvent, pH, and ionic strength conditions *(35)*. Such a flexibility also influences its adsorption characteristics on solids and in turn affects the subsequent suspension behavior. Using a fluorescent labelled polymer and by monitoring the extent of excimer formation it was shown that the polymer at the interface could have a stretched or coiled conformation at the interface depending on the pH. The rationale behind the use of this technique is the observation that the extent of excimer formation which depends on the interaction of an excited state pyrene pendant group of the polymer with another pyrene group in the ground state and therefore depends on the polymer conformation. This may be understood by examining Figure18 which shows that at low pH, there is a better probability for intramolecular excimer formation between pyrene groups resulting from a favorable coiled conformation. Similarly a low probability for the excimer formation at high pH may be understood as a consequence of the repulsion between the highly ionized carboxylate groups in the polymer and the subsequent stretching of the polymer chain. This difference is reflected in the nature of their fluorescence spectra as seen in Figure 19 where at low pH the intensity due to the excimer emission is larger than at higher pH.

We have also performed a detailed investigation on the flocculation behavior of alumina particles with and without added polymer under fixed and shifted pH conditions. The polymer conformation was shown to be a controlling factor of the

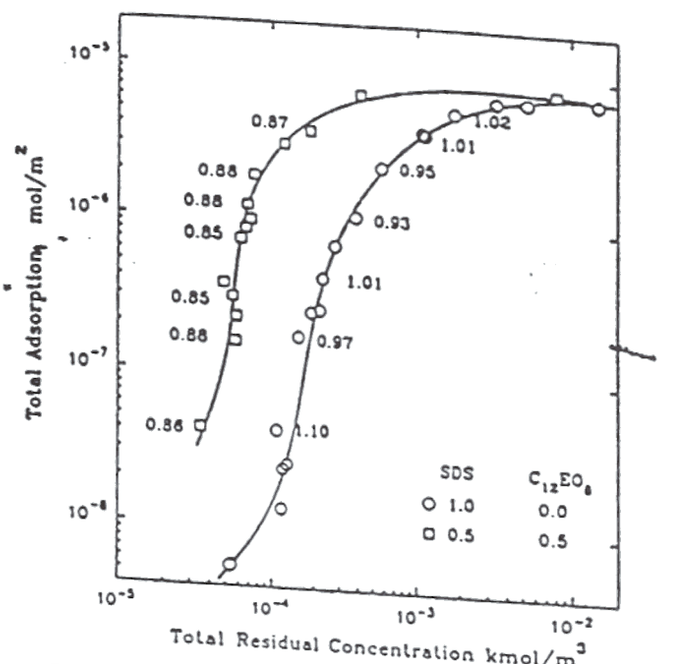

Figure 17. Polarity parameter of pyrene in the adsorbed layer of SDS/$C_{12}EO_8$ mixture on alumina.

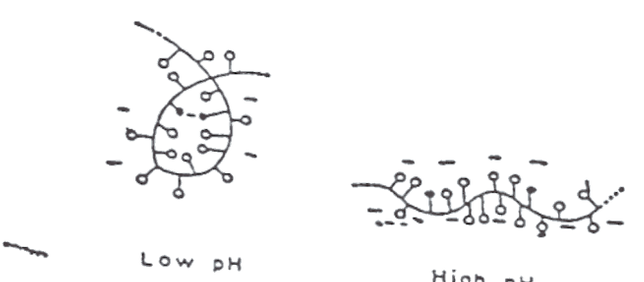

Figure 18. Schematic representation of the conformation of polyacrylic acid at different pH values. (Adapted from ref. 36)

flocculation process in this case. The results of fluorescence emission studies using pyrene labelled PAA in the adsorbed state under shifted pH conditions i.e. adsorbing the polymer at a fixed pH and then changing the pH to a desired value showed that the excimer fluorescence emission intensity of the polymer at the solid/liquid interface after adsorption at high pH values remains the same even after changing the pH to lower values (Figure 20). From this observation the variation of polyacrylic acid conformation at the solid-liquid interface under shifted pH conditions may be represented as shown in Figure 21. It may be inferred that the polymer conformation at a given pH may be manipulated by controlling the adsorption conditions *(36)*. In contrast, the polymer adsorbed in the coiled form at low pH did stretch out when the pH was increased.

Dapral at Solid-Liquid Interface. Hydrophobically modified polymers have been increasingly used nowadays to increase the viscosity and elasticity of solutions as they can undergo interesting intramolecular and intermolecular association by hydrophobic interactions. These polymers are also promising as steric stabilizers as well as flocculating agents for hydrophilic and hydrophobic surfaces in both aqueous and non-aqueous media. We have studied the stabilization effects of Dapral GE 202 (maleic anhydride α-olefin copolymer with both hydrophobic and hydrophilic side chains) which is a hydrophobically modified comb-type polymer whose structure is as indicated in Figure 22. The observed changes in suspension stability cannot be explained in terms of the corresponding changes in electrokinetic properties *(37)*. Fluorescence studies were conducted using free pyrene as the probe and the polarity parameter measured at different levels of Dapral adsorption (Figure 23). At low concentrations the I_y/I_t value for pyrene is similar to that in water but with increase in concentration this increases reaching upto a value of 1 at a Dapral concentration of 500 ppm. These suggest the formation of aggregates at the interface with the creation of hydrophobic microdomains into which the pyrene partitions preferentially. Such an aggregation can explain the continued adsorption of Dapral even after the reversal of surface charge. The formation of such hydrophobic aggregates would now render the surfaces hydrophilic since the ethylene oxide chains will be dangling into solution and stabilization of the suspension in this case is attributed to a combination of electrostatic repulsion and steric hindrance of the adsorbed molecules.

Fluorescence spectroscopy was also used to detect the orientation of Dapral on alumina particles in non-aqueous media*(38)*. 7-dimethylamino-4-methyl coumarin which is a relatively hydrophilic molecule was used to probe the adsorbed layer of DAPRAL at the alumina/toluene interface. The spectrum for the probe in the absence of DAPRAL is similar to that obtained in water solution (maximum emission at 470 nm, Figure 24). This is attributed to the hydrophilicity of the bare alumina surface. With an increase in polymer adsorption, the maximum wavelength shifts towards the shorter wavelength range reaching the value for hydrocarbon solvents (390 nm) at 500 mg/l of DAPRAL (Figure 25). This observation supports the mechanism of polymer adsorption through the interaction between the ethylene oxide chains and the hydroxyl groups on the alumina surface with the hydrocarbon side chains dangling towards the solution and the alumina particles eventually fully covered to become totally hydrophobic. This is supported by the fact that the alumina suspensions are stabilized significantly by the adsorption of DAPRAL.

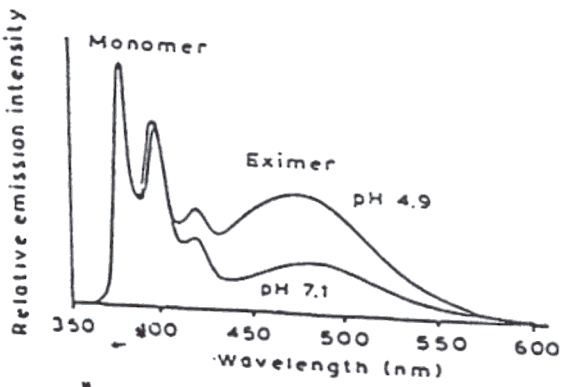

Figure 19. Schematic representation of the correlation of the extent of excimer formation and intrastrand coiling of pyrene labeled polyacrylic acid. (Adapted from ref. 36)

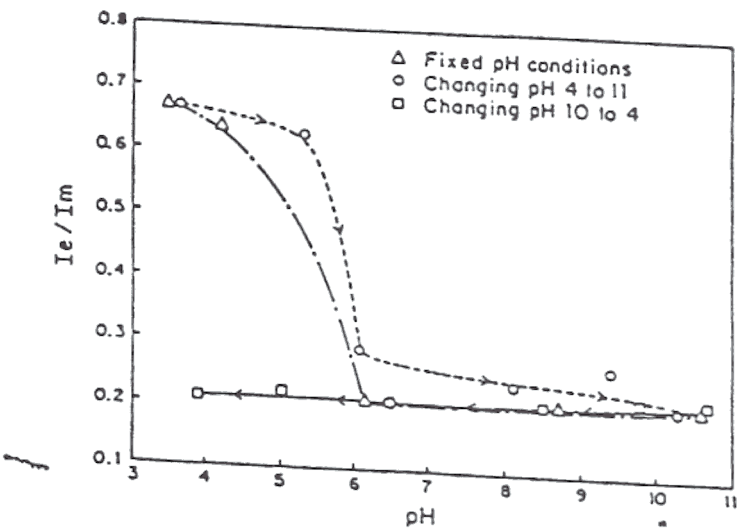

Figure 20. Excimer to monomer ratio, I_e/I_m for alumina with 20 ppm PAA as a function of final pH under changing pH conditions.

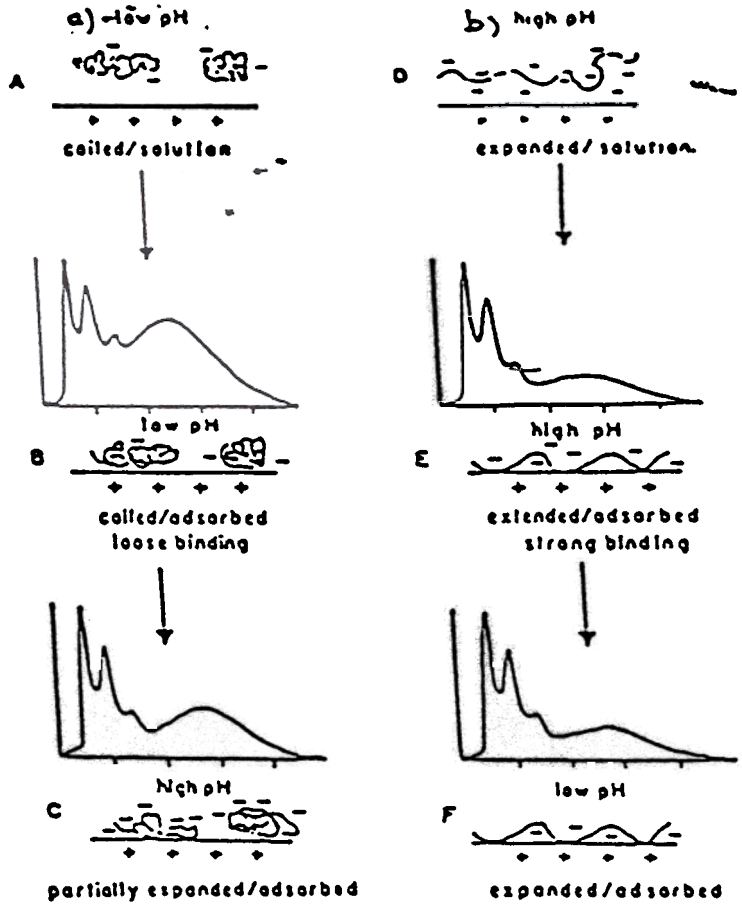

Figure 21. Schematic representationof the adsorption process of pyrene-labeled polyacrylic acid on alumina A) At low pH polymer is coiled in solution which leads to B) adsorption in coiled form. C) Subsequent raising of the pH causes some expansion of the polymer D) Polymer at high pH in solution is extended and binds E) strongly to the surface in this conformation F) Subsequent lowering of pH does not allow for sufficient intrastrand interactions for coiling to occur. (Adapted from ref. 36)

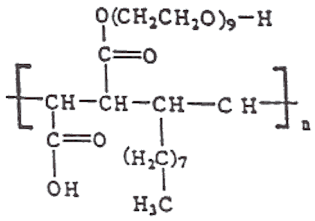

Figure 22. Molecular structure of DAPRAL.

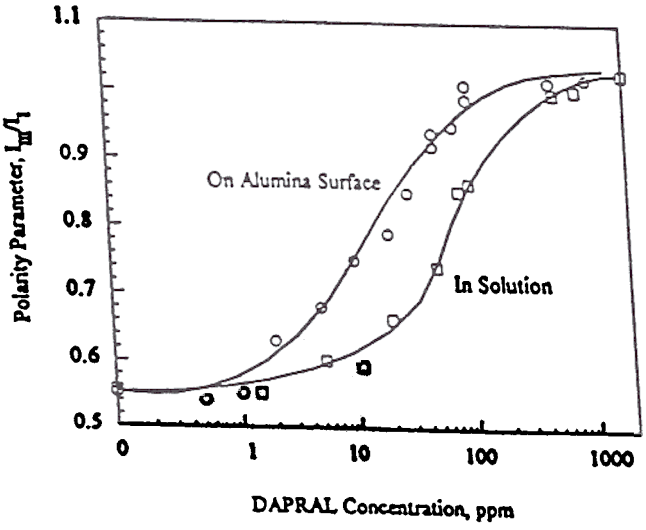

Figure 23. Aggregation of Dapral in solution and at the alumina-water interface (pH 8):(a) in solution, (b) at the interface. (Reproduced with permission from ref. 38. Copyright 1994, Elsevier)

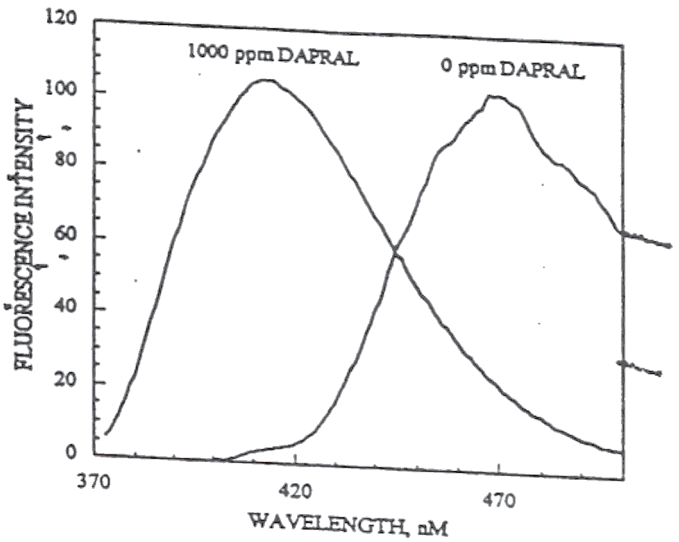

Figure 24. Fluorescence spectrum of 7-amino 4-methyl coumarin at the alumina toluene interface in the presence of 0 ppm DAPRAL and 1000 ppm DAPRAL. (Reproduced with permission from ref. 38. Copyright 1994, Elsevier)

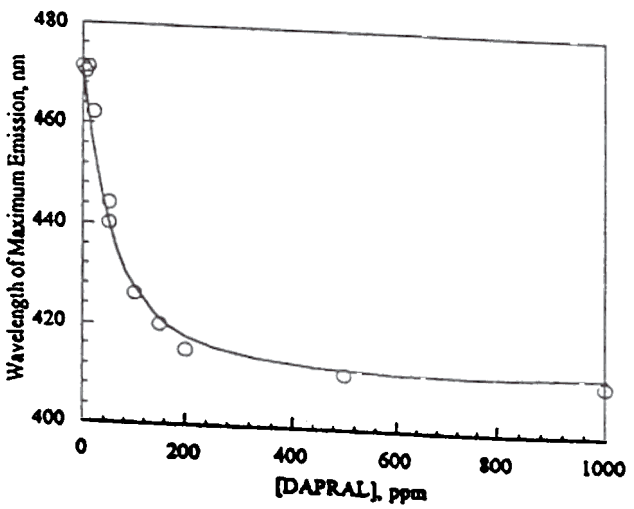

Figure 25. Diagaram illustrating the shift in maximum emission wavelength of coumarin at the alumina-toluene interface with adsorption of DAPRAL. (Reproduced with permission from ref. 38. Copyright 1994, Elsevier)

Polymer/Surfactant/Solid System

Polymer-Surfactant Aggregates at an Interface. Investigations on polymer-surfactant aggregates are of importance owing to the use of these mixed systems in areas related to enhanced oil recovery, colloidal stability, flotation and flocculation. The conformation of polyethylene oxide (PEO) mixed with sodium dodecysulfate at alumina-water interface was measured using pyrene-labeled polymer. Figure 26 shows the I_1/I_m values of the PyPEO on alumina surface preadsorbed with SDS. Interestingly, the conformation of the co-adsorbed PEO was markedly influenced as a result of its interaction with SDS *(39)*. Thus PEO could be force-adsorbed onto alumina. This experiment demonstrates the potential of fluorescence spectroscopy to investigate the conformational aspects of polymers and surfactants adsorbed together at a solid-liquid interface.

Concluding Remarks

A new insight has been obtained on the structure and evolution of surfactant and polymer aggregates at solid-liquid interfaces both in aqueous and non-aqueous media by the application of spectroscopic and classical methods. These findings have been correlated with the performance parameters of the individual systems. The aggregation number of sodium dodecylsulfate on alumina was determined at various points of the solloid evolution and the variation of the micro-viscosity within the solloid layer was determined along the isotherm using ESR and Raman spectroscopy. Fluorescence spectroscopic studies also indicate that steric hindrance to packing in the adsorbed layers controls the solloid formation of the alkyl xylenesulfonates. Also infrared spectroscopy has been used to study the adsorption of surfactants such as oleate on mineral surfaces. Pyrene probing revealed the solloidal structure of mixed surfactants. The effect of pH dependent conformational equilibria of polyacrylic acid on the adsorption process and its implications to flocculation have been explored to suggest reasonable conformational structures for the polymer solloid. The spectroscopic techniques were also useful in studying adsorption processes in non-aqueous media. Thus, the role of water in controlling the dispersion properties of alumina dispersed in cyclohexane by increasing the lateral diffusion of the adsorbed surfactant molecules was depicted using ESR technique. A rare insight has been gained on the stabilization of solids by the hydrophobically modified polymer Dapral in aqueous and non-aqueous media. Furthermore, spectroscopic methods were adopted to interrogate more complex systems consisting of surfactants and polymers. It is clear that there is a variety of techniques now becoming available to examine structures insitu at levels smaller than ever before and one can obtain valuable equilibrium and kinetic information on a molecular level by adapting these techniques suitably.

Acknowledgments. We wish to acknowledge the financial support from National Science Foundation, Department of Energy, Unilever Research and Nalco.

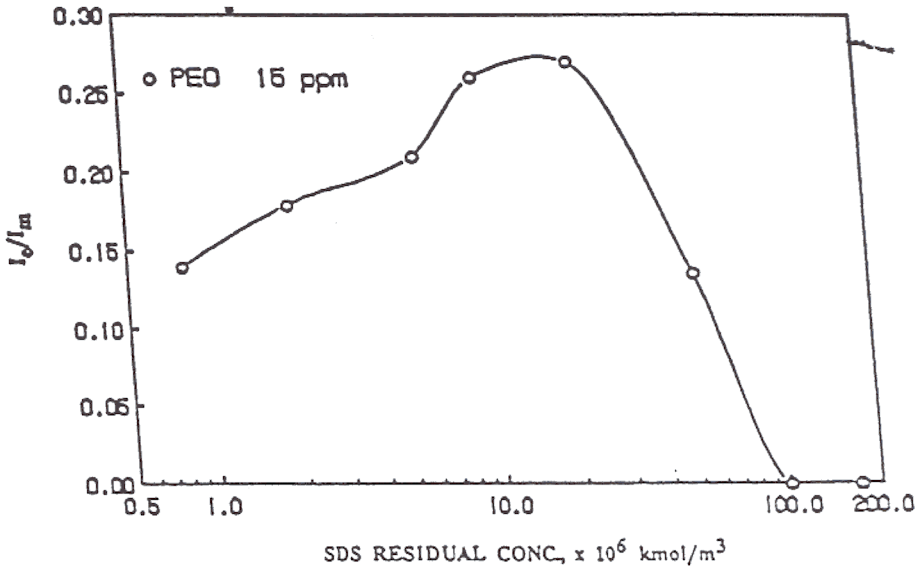

Figure 26. PEO conformation on the alumina surface preadsorbed with SDS expressed as coiling index. (Reproduced with permission from ref. 39. Copyright 1990, John Wiley & Sons)

Literature Cited

1. Hanna, H.S.; and Somasundaran, P., In D.O. Shah and R.S. Scheter (Eds.), Improved Oil Recovery by Surfactant and Polymer Flooding, Academic Press, New York, 1977, p 253.

2. Lakowicz, J.R.; "Principles of Fluorescence Spectroscopy", Plenum Press, New York, 1983.

3. Thomas, J.K.; "The Chemistry of Excitation at Interfaces", *American Chemical Society Monograph*, 1984.

4. Turro, N.J.; Cox, G.S.; Paczkowski, M.A.; "Photochemistry in Micelles", *Topics in Current Chemistry*, 1985, *129*, p 57

5. Demas, J.N.; "Excited State Lifetime Measurements", Academic Press, New York, 1983.

6. Wertz, J.H.; Bolton, J.R.; "Electron Spin Resonance - Elementary Theory and Practical Applications", Chapman and Hall, New York, 1986 .

7. Ranby, B.; "ESR Spectroscopy in Polymer Research", Rabek and Springer (eds), Berlin, 1977.

8. Francesca Ottaviani. M.; Bagiloni. P.; and Martini. G.; *J. Phys. Chem.*, 1983, *87*, p 3146.

9. Lim. Y.Y.; and Fendler. J.H.; *J. Am. Chem. Soc.*, 1978, *24*, p 7490.

10. Krishnakumar, S.; Somasundaran, P.; *J. Coll. & Int. Sci.*, 1994, *162*, p 425.

11. Barelli, A.; and Eicke, H. F.; *Langmuir*, 1986, *2*, p 780.

12. "Laboratory Methods in Vibrational Spectroscopy", Wills, H.A.; vander Maas, J.H.; Miller, R.C.G.;(Eds), John Wiley & Sons, New York, 1987.

13. Kellar, J.J.; Cross, W.M.; Miller, J.D.; *Applied Spectroscopy*, 1990, *44*, p 1508.

14. Kunjappu, J.T.; Somasundaran, P.; *J. Indian Chem. Soc.*, 1989, *66*, p 639.

15. Somasundaran, P.; PhD Thesis, University of California, Berkeley, 1964.

16. Somasundaran, P.; Feurstenau, D.W.; *J. Phys. Chem.*, 1966, *70*, p 90.

17. Somasundaran, P.; Kunjappu, J.T.; *Colloids & Surfaces*, 1989, *37*, p 245.

18. Harwell, J.H.; Bitting, D.; *Langmuir*, 1987, *3* , p 500.

19. Gaudin, A.M.; Feurstenau, D.W.; *Min. Eng.*, 1955, *7*, p 66.

20. Somasundaran, P.; Chandar, P.; Turro, N.J.; , *J. Coll. & Interface Sci.*, 1987, *117*, p 31.

21. Somasundaran, P.; Chandar, P.; Turro, N.J.; *Colloids & Surfaces*, 1986, *20*, p 145.

22. Somasundaran, P.; Chandar, P.; Chari. K.; *Colloids & Surfaces*, 1983, *8*, p 121.

23. Waterman, K.C.; Turro, N.J.; Chandar, P.; Somasundaran, P.; *J. Phys. Chem.*, 1986, *90*, p 6829.

24. Chandar, P., Somasundaran, P.; Waterman, K.C.; Turro, N.J.; *J. Phys. Chem.*, 1986, *91*, p 150.

25. Somasundaran, P.; Kunjappu, J.T. ; Kumar, C.V.; Turro, N.J.; Barton, J.K.; *Langmuir*, 1989, *5*, p 215.

26. Sivakumar, A.; Somasundaran, P.; *Langmuir*, 1994, *10*, p 131.

27. Malbrel, C.A.; D. Eng Sci. Thesis, Columbia University , 1991

28. Malbrel, C.A.; Somasundaran, P.; *Langmuir*, 1992, *8*, p 1285.

29. Krishnakumar, S.; Somasundaran, P.; *Langmuir*, 1994, *10*, p 2786.

30. Xiao, L.; Viswanathan, K.V.; Somasundaran, P.; In Extractive Metallurgy and Material Science, S. Li (ed.), Changhsha, China, 1987, p 110.

31. Harwell, J.H.; Scamehorn, J.F.; In Mixed Surfactant Systems, Ogino,K., Abe, M., (eds), Surfactant Science Series, Vol 33, Marcel Dekker, New York, 1993, p 263.

32. Ogino, K.; Abe, M.; *J. Coll. & Interface . Sci.*, 1985, *107*, p 509.

33. Sivakumar, A.; Somasundaran, P.; Thach, S.; *Colloids & Surfaces*, 1993, *70*, p 69.

34. Morawetz, H.; "Macromolecules in Solution", John Wiley & Sons, New York, 1975.

35. Arora, K.S.; Turro, N.J.; *J. Polymer Science*, 1987, *25* , p 243.

36. Chandar, P.; Somasundaran, P.; Waterman, K.C.; Turro, N.J.; *Langmuir*, 1987, *3* , p 298.

37. Somasundaran, P.; Li, C.; XiangYu ; *Colloids & Surfaces*, 1992, *69*, p 155.

38. Somasundaran, P.; Xiang Yu; *Colloids & Surfaces*, 1994, *89*, p 277.

39. Maltesh, C.; Somasundaran, P.; Ramachandran, R.; *J. Applied Polymer Science*, 1990, *45*, p 329.

RECEIVED July 27, 1995